TISSUE ENGINEERING: Part A
Volume 21, Numbers 5 and 6, 2015
© Mary Ann Liebert, Inc.
DOI: 10.1089/ten.tea.2014.0001

# Effects of BMP-12-Releasing Sutures on Achilles Tendon Healing

Connie S. Chamberlain, PhD,[1] Jae-Sung Lee, PhD,[1] Ellen M. Leiferman, DVM,[1] Nicholas X. Maassen, MD,[1] Geoffrey S. Baer, MD, PhD,[1] Ray Vanderby, PhD,[1,2,*] and William L. Murphy, PhD[1,2,*]

Tendon healing is a complex coordinated event orchestrated by numerous biologically active proteins. Unfortunately, tendons have limited regenerative potential and as a result, repair may be protracted months to years. Current treatment strategies do not offer localized delivery of biologically active proteins, which may result in reduced therapeutic efficacy. Surgical sutures coated with nanostructured minerals may provide a potentially universal tool to efficiently incorporate and deliver biologically active proteins directly to the wound. Additionally, previous reports indicated that treatment with bone morphogenetic protein-12 (BMP-12) improved tendon healing. Based on this information, we hypothesized that mineral-coated surgical sutures may be an effective platform for localized BMP-12 delivery to an injured tendon. The objective of this study was, therefore, to elucidate the healing effects of mineral-coated sutures releasing BMP-12 using a rat Achilles healing model. The effects of BMP-12-releasing sutures were also compared with standard BMP-12 delivery methods, including delivery of BMP-12 through collagen sponge or direct injection. Rat Achilles tendons were unilaterally transected and repaired using BMP-12-releasing suture (0, 0.15, 1.5, or 3.0 μg), collagen sponge (0 or 1.5 μg BMP-12), or direct injection (0 or 1.5 μg). By 14 days postinjury, repair with BMP-12-releasing sutures reduced the appearance of adhesions to the tendon and decreased total cell numbers. BMP-12 released from sutures and collagen sponge also tended to improve collagen organization when compared with BMP-12 delivered through injection. Based on these results, the release of a protein from sutures was able to elicit a biological response. Furthermore, BMP-12-releasing sutures modulated tendon healing, and the delivery method dictated the response of the healing tissue to BMP-12.

## Introduction

Tendon healing is a complex coordinated series of overlapping events orchestrated by numerous biologically active proteins. Unfortunately, tendons have limited regenerative potential and repair may be protracted months to years. Complete recovery without scar is virtually never attained, and results in other musculoskeletal morbidities. To accelerate healing, numerous delivery methods of therapeutic proteins/growth factors to the injury have been tested.

For tendon healing, translation of therapeutic proteins (e.g., cytokines, growth factors) to clinical applications has numerous challenges. Current strategies for protein treatments often rely on bolus delivery through injection or collagen sponge. This rapid protein release does not control delivery kinetics and may reduce the therapeutic efficacy, since the proteins may be more effective when delivered in a sustained manner.[1,2] Common strategies to control protein release range from polymer scaffolds to injectable micro- and nanoparticles. While these strategies can control protein release kinetics, maintenance of protein biological activity remains a challenge,[3] and the devices are not amenable to inclusion in many clinical scenarios. Another strategy entails delivery of biologically active proteins from commonly used medical devices that are present within, or adjacent to, a surgical wound.

Surgical sutures serve as a ubiquitous medical device to link distinct portions of a surgical wound and may also represent ideal delivery platforms for therapeutic proteins due to their proximity to damaged tissue. These desirable aspects have led investigators to develop sutures that deliver synthetic drugs[4,5] and therapeutic proteins[5–8] to enhance healing. Previous results from our lab demonstrated the ability to control the release of therapeutic proteins from sutures without significantly affecting the inherent suture properties.[5,9] A primary component of the approach involved coating the suture surface with a nanoporous calcium phosphate (CaP) mineral layer, which served as a mediator of binding and controlled the release of biologically active proteins.

Departments of [1]Orthopedics and Rehabilitation and [2]Biomedical Engineering, University of Wisconsin, Madison, Wisconsin.
*These authors are equal contributors to this article and will serve as corresponding authors.

Calcium phosphate minerals have been commonly used for bone tissue repair due to their similar composition to bone mineral. However, due to its remarkable ability to bind biological molecules, CaP has been a subject of growing interest in therapeutic delivery strategies. Similar to hydroxyapatite chromatography, CaP minerals bind through charge–charge interactions to various biological molecules, including proteins,[10,11] peptides,[12] and nucleic acids.[13,14] This biomolecule–CaP affinity provides a potentially universal tool to efficiently incorporate within delivery carriers. Indeed, previous results have shown that growth factors, including bone morphogenetic protein 2 (BMP-2),[15] transforming growth factor-beta 1 (TGF-β1),[16] insulin-like growth factor 1 (IGF-1),[17] and fibroblast growth factor 2 (FGF-2),[18] and other therapeutic agents, such as metal ions for antimicrobial purposes,[19,20] can be surface bound during the formation of CaP cements or coprecipitated during growth of CaP coatings in modified simulated body fluids (mSBF), and can achieve sustained release as the biomineral is resorbed without negatively impacting handling and surgical applicability.

In this study, we particularly focused on delivery of BMP-12 for tendon repair. BMPs are a family of highly related molecules that are members of the TGF-β superfamily. Most BMPs induce bone and cartilage formation in animals by influencing the differentiation of mesenchymal progenitor cells to a cartilage or bone lineage.[21,22] However, BMP-12 (alternatively, GDF-7) is involved in tendon differentiation and maintenance. Previous studies indicated that BMP-12 treatment induced ligament and tendon-like structures, *in vivo*.[23,24] Additionally, BMP-12 gene transfer into a complete tendon laceration model increased tensile strength and stiffness of repaired tendons by twofold, indicating improved tendon healing.[25] *In vitro* studies further showed that rhBMP-12 increased procollagen type I and type III expression in human tendon fibroblasts.[26] Based on these results, BMP-12 may play a significant role in tendon healing by modulating collagen formation and tendon remodeling. In this study, we present an experiment where BMP-12 is incorporated within a nanoporous mineral coating on a surgical suture and used for *in vivo* tendon injury repair. Due to the beneficial properties of surgical sutures and the utility of CaP minerals as a delivery vehicle, we hypothesized that mineral-coated surgical sutures may be an effective platform for localized and sustained BMP-12 delivery to the injured Achilles tendon. Therefore, the healing effects of mineral-coated sutures releasing BMP-12 were elucidated using a rat Achilles healing model. The effects of BMP-12-releasing sutures were further compared with standard clinical BMP-12 delivery methods, including delivery through collagen sponge or direct injection.

## Materials and Methods

### *Preparation of mineral-coated sutures*

Five types of sutures exhibiting different material, construction, and size characteristics (Table 1) were initially tested for mineral coating capabilities and included Vicryl, Prolene, Mersilene, Ethibond Excel (all from Ethicon, Somerville, NJ), and Polysorb (Coviden, Mansfield, MA) sutures. Sutures (USP 5-0; Ethicon, Somerville, NJ) were coated with CaP by incubating in mSBF (141 mM NaCl, 4 mM KCl, 0.5 mM $MgSO_4$, 1.0 mM $MgCl_2$, 4.2 mM $NaHCO_3$, 5.0 mM $CaCl_2$, 2.0 mM $KH_2PO_4$, 20 mM Tris base). The sutures were cut into 15 cm lengths and incubated in mSBF at 37°C, pH 6.8 for 7 days under mild rotation. The mSBF solution was refreshed daily to keep the ionic concentrations constant during incubation. After incubating in mSBF, the resulting sutures were then rinsed with deionized water and lyophilized. The surface morphology of mineral coating created on sutures was observed using the scanning electron microscopy (SEM, LEO 1530 field emission SEM; Zeiss, Jena, Germany). The compositional characteristics of the coated Vicryl sutures ($n = 3$ sutures) were further examined by the Fourier transform infrared (FT-IR) spectroscopy (Equinox 55 spectrometer; Bruker AXS, Karlsruhe, Germany) and energy dispersive spectroscopy equipped on SEM. X-ray diffraction spectroscopy (XRD) was performed to identify the crystal structure of the resulting mineral coating using the Hi-Star 2-D X-ray diffractometer (Bruker AXS, Madison, WI).

Table 1. Surgical Sutures of Various Size, Construction and Material Characteristics, Tested for Mineral Coating Capabilities

| *Suture* | *Material* | *Size* | *Absorbable* | *Construction* |
|---|---|---|---|---|
| Vicryl | Polyglactin 910 | 6-0 | Yes | Braided |
| Ethibond Excel | Polyester/ Dacron | 4-0 | No | Braided |
| Prolene | Polypropylene | 4-0 | No | Monofilament |
| Mersilene | Polyester/ Dacron | 5-0 | No | Braided |
| Polysorb | Glycolide/ Lactide | 4-0 | Yes | Braided |

### *Protein binding to mineral coating*

Time required for protein binding to mineral coating was first assessed by measuring the amount of cytochrome c binding to the mineral-coated scaffold. Cytochrome c was chosen because it is a soluble protein with a molecular weight and isoelectric point similar to several growth factors. Mineral-coated poly(lactic-*co*-glycolic acid) (PLGA) was incubated in phosphate buffered saline (PBS) containing 100 or 500 μg/mL cytochrome c for 1, 2, 3, or 4 h. A control group of 100 and 500 μg/mL cytochrome c without exposure to mineral coating was also included and served as the control. Samples ($n = 3$–4) were used for micro-BCA analysis to estimate the amount of cytochrome c binding based on the change in protein concentration after mineral-coated scaffold incubation.

### *Incorporation of BMP-12 into mineral-coated suture*

Based on previous protein release studies[5,27] the CaP-coated Vicryl sutures were incubated in BMP-12 (Pfizer, Cambridge, MA) solution to allow for BMP-12 adsorption on the mineral surface. The gas-sterilized sutures were incubated in BMP-12 solutions (0.1, 1.0 and 2.0 μg/mL) at 37°C for 4 h before animal surgery.

### *BMP-12 experimental model*

Experimental procedures were approved by the University of Wisconsin Institutional Animal Care and Use

Table 2. Treatment Groups and Number of Animals for the *In Vivo* Repair of Achilles Tendon

| *Treatments for Achilles tendon repair* | *Rat No.* |
|---|---|
| Mineral-coated suture + No BMP-12 (Blank) | 3 |
| Mineral-coated suture + 0.15 μg BMP-12 (0.15 μg BMP) | 3 |
| Mineral-coated suture + 1.5 μg BMP-12 (1.5 μg BMP) | 3 |
| Mineral-coated suture + 3.0 μg BMP-12 (3.0 μg BMP) | 3 |
| Mineral-coated suture and 1.5 μg BMP-12 SC injection (BMP Injection) | 3 |
| Mineral-coated suture PBS SC injection (PBS Injection) | 3 |
| Collagen sponge + No BMP-12 (Sponge) | 3 |
| Collagen sponge + 1.5 μg BMP-12 (BMP Sponge) | 3 |
| Total rat Achilles | 24 |

BMP, bone morphogenetic protein; PBS, phosphate buffered saline.

Committee. To identify the influence of BMP-12 on Achilles tendon healing, 24 skeletally mature male Wistar rats (275–299 g) were utilized for this study (3 rats per treatment group; Table 2). Rats were randomly divided into equal groups and subjected to unilateral Achilles tendon transection. Tendons were transected, rather than torn, to create uniform defects for healing. A 3 cm long incision was made over the Achilles tendon. The Achilles and superficial digital flexor (SDF) tendons were exposed and dissected from the surrounding tissues. The SDF tendons were separated from the Achilles and surgically removed. The Achilles tendon was transected in the midsubstance of the tendon (half way between the calcaneal insertion and the musculotendinous junction) and the tendon ends were reappositioned and repaired using a Krackow locking loop stitch, in which two locking loops were placed on each side of the tendon, with 5-0 absorbable Vicryl suture. The experimental sutures were: mineral coated (Blank) alone (serving as the control) or mineral-coated sutures releasing 0.15 μg BMP-12, 1.5 μg BMP-12, or 3.0 μg BMP-12 (Table 2). To compare the effects of BMP-12 released from the suture to a single injection of BMP-12, another set of injured Achilles tendons were repaired with mineral-coated sutures. These animals were then subcutaneously administered 1.5 μg of BMP-12 or PBS (serving as the vehicle control). Injections were made subcutaneously near the injury, but not directly over the sutures to avoid possible binding of BMP-12 to the mineral-coated sutures. To further compare the effects of BMP-12 released from sutures with a standard protein delivery method, another set of Achilles tendons were repaired with collagen sponge. In this study, after rats underwent Achilles tendon transection, the Achilles were repaired with uncoated 5-0 vicryl sutures and collagen sponge containing 1.5 μg BMP-12 or PBS (vehicle control). After repair of the tendon, muscular and dermal tissue layers were closed with 4-0 Dexon suture and skin staples, respectively. Following transection and repair of the Achilles tendon, the joint was immobilized internally using a wire cerclage. A 4 mm diameter hole was drilled in the tuber calcaneus and 2-0 stainless steel surgical suture was passed proximally, through the fibula–tibia fork, and distally through the hole in the tuber calcaneus. The wire ends were then twisted together and tightened, placing the hock in full extension. The skin was sutured closed after insertion of the cerclage. After surgery, rats were able to maintain normal cage activity. Rat ambulation was monitored by a trained observer for 7 days thereafter. All rats were mobile within 30 min of anesthesia removal after surgery. At 14 days postinjury animals were euthanized and tendons were measured, collected, and weighed. Tendons were carefully dissected and immediately embedded longitudinally, in an optimal cutting temperature medium for liquid nitrogen flash freezing and used for histology and immunohistochemistry (IHC).

### *Macroscopic analysis*

At the time of tissue collection, the tendon and tissue surrounding the tendon was observed for changes in vascularity and inflammation. Adhesions between the tendon and surrounding area tissue were also reported. Observations were ranked based on a scale of 0–3 (0 = none, 1 = mild; 2 = moderate; and 3 = severe). Tendon weight, length, and granulation tissue size were also measured.

### *Immunohistochemistry*

To identify cellular and extracellular matrix (ECM) changes within the healing tendon, IHC and histology were performed. Longitudinally positioned cryospecimens were serially sectioned (5 μm thickness), ensuring the center of the defect was mounted on each Colorfrost Plus (Fisher Scientific, Pittsburgh, PA) microscope slides, and maintained at −80°C. IHC was performed on frozen cryosections using mouse monoclonal antibodies. Cryosections were fixed in acetone, exposed to 3% hydrogen peroxide to remove endogenous peroxidase activity, blocked with Background Buster (Innovex Biosciences, Richmond, CA), and incubated with the primary antibodies. Mouse monoclonal antibodies to CD31 (1:100; Abcam-Serotec, Raleigh, NC), α-smooth muscle actin (1:100; Dako, Carpinteria, CA), and Ki-67 (1:25; Dako) were used to identify the endothelial cells/blood vessel lumen, myofibroblasts, and proliferating cells, respectively. Mouse antibodies were also used to identify type I procollagen (straight; SP1.D8; Developmental Hybridoma, Iowa City, IA) and the scar indicator, type III collagen (1:8000; Sigma-Aldrich, St. Louis, MO). Sections were then incubated with biotin, and streptavidin-conjugated to horseradish peroxidase using the Stat Q IHC staining kit (Innovex Biosciences, Richmond, CA). The bound antibody was then visualized using diaminobenzidine (DAB). Stained sections were dehydrated, cleared, cover-slipped, and visualized using light microscopy. After staining, images of each IHC marker were collected using a camera-assisted microscope (Nikon Eclipse microscope, model E6000 with an Olympus camera, model DP79). Within each IHC-stained tissue section, three images were captured (at 400× magnification) within each selected area, including, around the suture, within the granulation tissue, and outside of the granulation tissue (ends) for a total of nine images per section. For each IHC stain, three sections were counted per rat for a total of 27 images. Images captured for measurement of granulation tissue size, endothelial cells, myofibroblasts, type I procollagen, and type III

collagen were quantified using the ImageJ (National Institutes of Health, NIH, Bethesda, MD). Images of blood vessel lumen and proliferating cells were quantified manually.

### *Histological analysis*

Achilles tendon sections were Hematoxylin and Eosin (H&E) stained to observe general morphology of the healing tendons. To identify total cells, sections were also stained with 4′,6-diamidino-2-phenylindole (DAPI). Finally, Alizarin Red staining was also performed to detect localization of mineral coating within the tendon. After staining, images were captured and used to measure granulation tissue size, mineral content (using a 40× magnification), and total cells (using 400× magnification) within the tendon using the ImageJ. Area of the granulation tissue was normalized to the total Achilles tendon area and expressed as the percent normalized granulation tissue. Obvious oblique sections were excluded from analysis.

### *Fractal analysis*

Tissue organization was quantified by the fractal dimension in the fashion of Frisch *et al.*[28] Before fractal analysis, H&E images were converted from grayscale to binary images using a threshold value that was automatically determined using the automatic graythresh command in MATLAB (Mathworks, Natick, MA). Fractal analysis of each binary image was performed using a MATLAB routine, which calculated the fractal dimension using the Minkowski–Bouligand dimension, also known as the box counting dimension.[29] A smaller fractal dimension was indicative of a more linearly organized tissue. We have previously reported the use of fractal analysis using the SEM and multiphoton microscopy.[28,30] To further corroborate the use of fractal analysis on H&E-stained sections, H&E images from the prior multiphoton study[28] were analyzed using fractal analysis. H&E images ($n = 3$ images/day) were obtained from medial collateral ligament at 5, 9, 11, 14, and 28 days postinjury (without any treatment) and subjected to fractal analysis. Data were fitted onto a curve using a second-order polynomial equation to determine the $R^2$ value.

### *Statistical analysis*

Data collected from the different Achilles tendon regions, within each experimental group, were averaged together and also subgrouped (granulation tissue, suture, outside of the granulation tissue), to identify any potential spatial differences of each factor measured. Pairwise Student's *t*-tests were performed between sponge and BMP-12 sponge groups as well as between PBS injection and BMP-12 injection groups. Suture data were subjected to analysis of variance (ANOVA) to examine treatment differences. If the

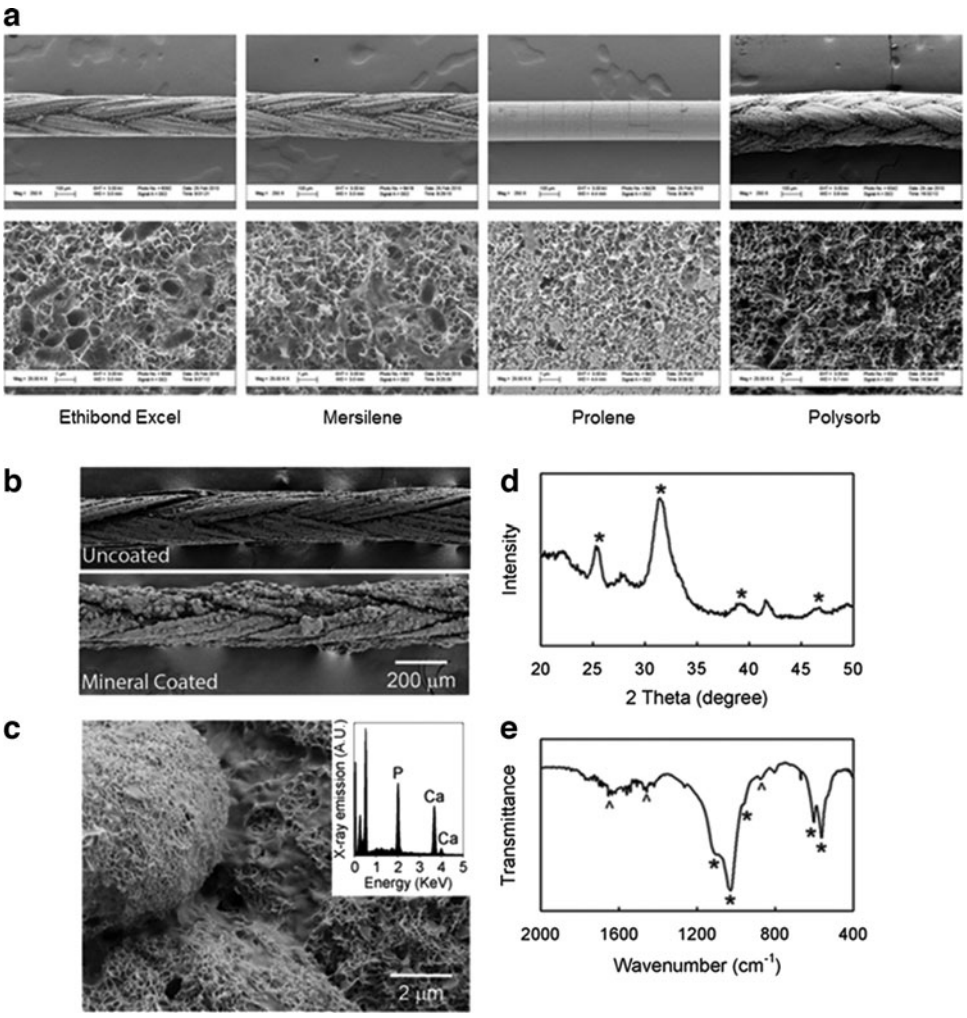


**FIG. 1.** Formation of mineral coating on surgical sutures. **(a)** Scanning electron microscopy (SEM) images of as-received Mersilene, Ethibond Excel, Proline, and Polysorb (*top panel*), and mineral-coated (*bottom panel*) surgical sutures indicating successful mineral coating on various types of sutures. **(b)** SEM images of as-received Vicryl suture (*top*) and mineral-coated (*bottom*) Vicryl suture. **(c)** SEM image and energy dispersive spectroscopy spectrum (*inset*) of calcium phosphate (CaP) coating surface. X-ray diffraction spectroscopy **(d,** * indicates the characteristic peaks of CaP**)** and Fourier transform infrared **(e,** * and ^ denote the peaks from phosphate and carbonate, respectively**)** spectra of CaP coating created on coated Vicryl.

overall $p$-value for the F-test in ANOVA was significant ($p < 0.100$), Scheffe's *post hoc* comparisons were performed. Scheffe's results were considered statistically significant if $p < 0.05$. Experimental results are presented as the means ± standard error of the mean. Computations were performed using the KaleidaGraph, version 4.03 (Synergy Software, Inc., Reading, PA).

## Results

### *CaP mineral coating characteristics*

For all sutures tested, mSBF incubation resulted in the formation of uniform CaP mineral coating on the entire suture surfaces (Fig. 1a, b), with characteristics consistent with a poorly crystalline, carbonate-substituted hydroxyapatite mineral phase. The coating displayed a nanoporous structure in electron micrographs (Fig. 1a–c) similar to prior studies from our group[31–34] and its ratio of calcium and phosphorus was 1.67 ± 0.03 (inset of Fig. 1c). Typical broad CaP peaks at 26°, 31°, 39°, and 46° appeared in the X-ray diffraction pattern (Fig. 1d) indicative of hydroxyapatite. FT-IR spectrum showed characteristic peaks associated with carbonate and phosphate (Fig. 1e). These results are similar to our previous mineral-coated suture publication reporting calcium and phosphorous ratios of 1.64 ± 0.10 and X-ray diffraction patterns with peaks at 26°, 31°, 39°, and 46°.[5] Collectively, SEM, XRD, and FT-IR spectra confirmed the formation of a reproducible nanoporous, carbonate-substituted, CaP coating. The successful mineral coating on all surgical sutures examined indicates broad applicability of the suture coating approach in clinical scenarios. Based on these findings, the braided, absorbable Vicryl sutures, which met our specific surgical specifications, were selected for the *in vivo* BMP-12 Achilles repair experiment.

### *Protein binding to mineral coating*

To determine the time required for protein binding, cytochrome c was added to the mineral-coated scaffold and protein concentration was quantified over time. At a concentration of 100 μg/mL, cytochrome c significantly bound to the mineral-coated scaffold by 1 h of exposure, as indicated by the decrease in protein concentration in solution ($p < 0.001$; Fig. 2). Incubation times beyond 1 h were not significantly different. In contrast, binding of 500 μg/mL cytochrome c to mineral coating also occurred within 1 h, but was not significantly different from the control until 4 h postincubation. These protein binding studies indicated the possible intraoperative use of protein-releasing mineral-coated devices within 1 h of preparation.

### *Mineral distribution within the tendon*

To determine the spatial localization of mineral coating remaining within the healing tendon, we stained with Alizarin Red, which stains calcium phosphate minerals red. This experiment was particularly performed to determine whether the mineral coating from the surgical suture remained within the healing region, or was instead removed from the suture location. The amount of coating found within the suture region, was not significantly different among treatment groups ($p = 0.907$; Fig. 3a, c), indicating that incubation with varying doses of BMP-12 did not alter the mineral content on the suture. However, the spatial localization of mineral within the tendon regions was significantly different ($p < 0.001$). Most of the mineral coating remained localized around the sutures, as indicated by the high density of positive Alizarin Red staining surrounding the suture ($11.31 \pm 1.39 \times 10^{-3}$ density/mm$^2$). Alizarin Red was also found in the granulation tissue ($6.42 \pm 1.15 \times 10^{-3}$ density/mm$^2$) and outside of the granulation tissue ($0.66 \pm 0.20 \times 10^{-3}$ density/mm$^2$), but in significantly lower amounts (Fig. 3b, c). These data indicate that the mineral coatings, which were loaded with BMP-12 in some conditions, remained largely localized near the sutures, as expected. Additionally, the minute amount of CaP coating the surgical suture surface would preclude any sort of potential ectopic bone formation.

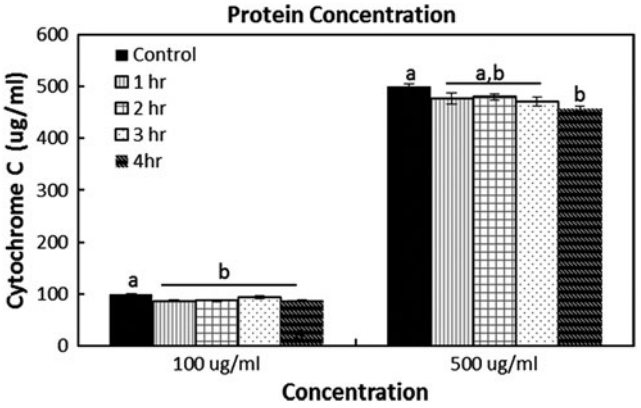


**FIG. 2.** Protein binding on mineral-coated device. Micro-BCA results quantifying the amount of 100 or 500 μg/mL cytochrome c remaining in solution before (Control) and after the addition of the mineral-coated scaffold. Samples were collected at 1, 2, 3, and 4 h postincubation. At 100 μg/mL cytochrome c, protein concentration decreased significantly from solution (indicating increased binding to mineral coating) within 1 h of exposure to mineral coating. Incubation beyond 1 h was not different. At 500 μg/mL cytochrome c, the amount of unbound protein was significantly reduced by 4 h. If analysis of variance (ANOVA) results were $p < 0.10$, Scheffe's *post hoc* pairwise analysis was performed. [a,b] Within the concentration indicates *bars* without a common *superscript letter* differ ($p < 0.05$). Values are expressed as mean ranking ± standard error of the mean (S.E.M.).

### *Macroscopic results*

To explore the effects of BMP-12 on the Achilles tendon and the tissue surrounding the tendon, macroscopic ranks and measurements were obtained at the time of tissue collection. Macroscopic rankings indicated that BMP-12-releasing sutures significantly ($p < 0.001$) altered surrounding area adhesions based on the dose of BMP-12 (Fig. 4a). Specifically, 1.5 μg (0.0 ± 0 rank) and 3.0 μg (2.0 ± 0.29 rank) of BMP-12-releasing sutures reduced adhesions compared with the blank (no BMP-12) suture (3.0 ± 0.0 rank), with 1.5 μg BMP-12-releasing sutures having the greatest effect. A dose of 1.5 μg BMP-12 (1.83 ± 0.17 rank) also decreased the surrounding area vascularity compared with the blank suture (3.0 ± 0.0 rank; Fig. 4b). Tendon inflammation, tendon vascularity, length, weight, or surrounding area inflammation was not significantly influenced

by BMP-12-releasing sutures ($p > 0.10$; data not shown). Similar to the suture results, delivery of BMP-12 by collagen sponge also reduced ($p = 0.040$) surrounding area adhesions, whereas BMP-12 injections did not (Table 3). In contrast, BMP-12 injections significantly increased the surrounding area vascularity ($p = 0.016$) and tendon inflammation ($p = 0.016$), whereas BMP-12-releasing collagen sponges did not ($p > 0.050$; Table 3).

### *Immunohistochemistry*

To determine if BMP-12 influenced the cellular profile, angiogenesis, or scar formation within the healing tendon, the total number of cells, proliferating cells, endothelial cells, blood vessel lumen, myofibroblasts, type III collagen, and type I procollagen were quantified. Total cell numbers were significantly reduced after the tendon was repaired with sutures releasing 3.0 μg (666.24 ± 39.84 cells/mm$^2$) BMP-12 ($p = 0.057$; Fig. 4c) when compared with blank (no BMP-12) sutures (822.33 ± 37.61 cells/mm$^2$). These differences were only noted away from the sutures (i.e., outside of the granulation/suture area). *Post hoc* analysis indicated that myofibroblasts were not significantly different within treatment groups after suture repair (Table 4), but was significantly decreased in conditions that released 1.5 μg BMP-12 from collagen sponge ($1.95 \pm 0.60 \times 10^{-3}$ density/mm$^2$) compared with sponge alone ($6.34 \pm 1.08 \times 10^{-3}$ density/mm$^2$; Table 5). Blood vessel lumen number was also increased after BMP-12 injection ($p = 0.033$; Table 5). No significant differences were found in the proliferating cells, endothelial cells, myofibroblasts, type III collagen, and type I procollagen after BMP-12 treatment regardless of delivery method (Tables 4 and 5).

### *Granulation tissue size and collagen organization*

Improved tendon healing is characterized by a reduced area in granulation tissue and enhanced collagen organization. Fractal analysis results indicated that collagen organization was not improved with BMP-12-releasing sutures (Table 4) or collagen sponge (Table 5). However, injection of BMP-12 (Table 5) significantly improved collagen organization compared with PBS injections ($p = 0.040$). Although collagen organization was improved through BMP-12 injections, normalized granulation tissue size was not changed by BMP-12, regardless of administration method (Tables 4 and 5 and Fig. 5). These results suggest that the passing of the mineral-coated surgical sutures did not cause any adverse intratendinous tendon damage. Based on these results, BMP-12 plays a greater role in modulating scar formation through ECM remodeling rather than through reducing the size of injury.

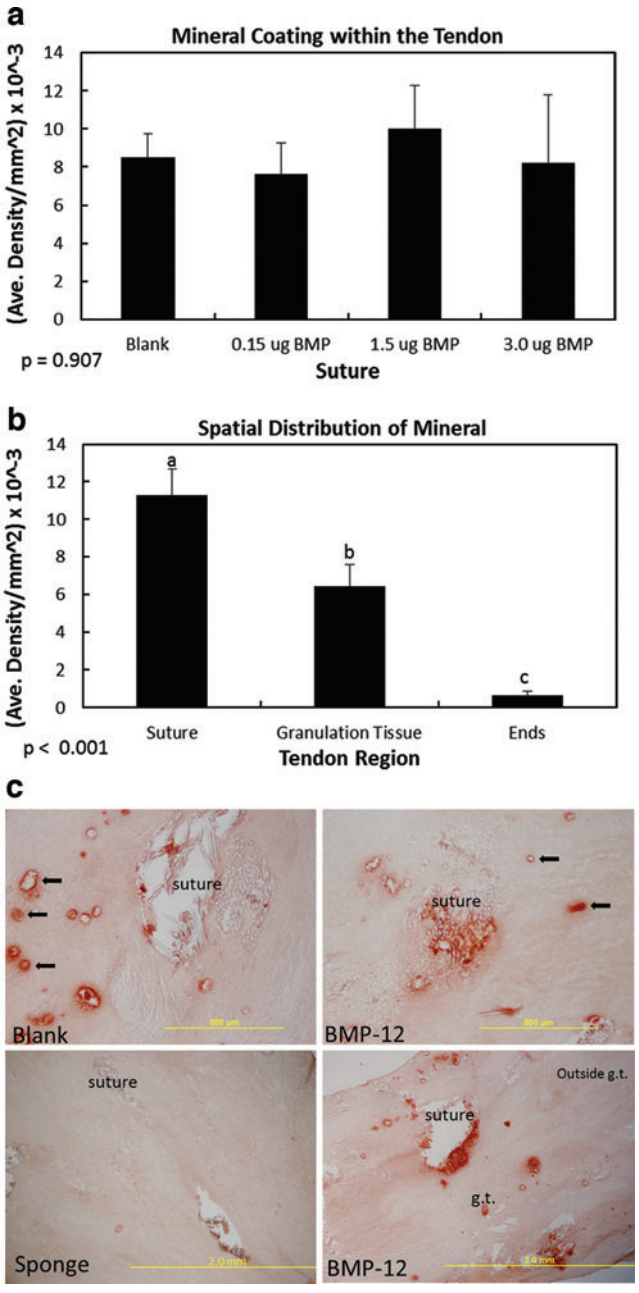


**FIG. 3.** Spatial localization of mineral coating within the day 14 Achilles tendon. Graphs showing **(a)** Alizarin Red results between treatment groups after Achilles tendon repair with mineral-coated sutures with or without bone morphogenetic protein 12 (BMP-12) **(a)**, the spatial distribution of mineral coating throughout the Achilles tendon **(b)**; and representative micrographs of Alizarin Red staining within the tendon after repair with mineral coating sutures **(c)**. Quantity of Alizarin Red, a stain for calcium, was similar among all treatment groups **(a)**. Mineral coating was primarily localized to the suture area **(b)**. Granulation tissue and the tendon ends (i.e., outside of the granulation tissue) also had measurable amounts of mineral, but were significantly lower than the suture area **(b)**. Representative micrographs of mineral-coated (*top left*), BMP-12-releasing sutures (*top right*), sponge (*bottom left*), and BMP-12-injected and mineral-coated suture repair (*bottom right*), indicating Alizarin Red-stained mineral coating within the tendon **(c)**. The sponge group represented a negative control for Alizarin Red staining. *Arrows* indicate areas positive for Alizarin Red staining. The *p*-value beneath the graph indicates ANOVA results. If ANOVA results were $p < 0.10$, Scheffe's *post hoc* pairwise analysis was performed. [a,b,c] Within a graph indicates *bars* without a common *superscript letter* differ ($p < 0.05$). Values are expressed as mean density ± S.E.M. Color images available online at www.liebertpub.com/tea

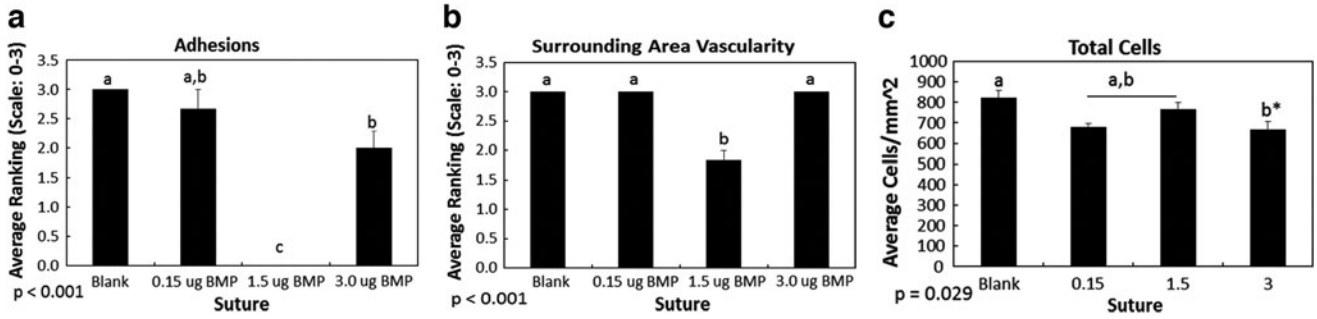


**FIG. 4.** Effect of BMP-12-releasing sutures on macroscopic results on the day 14 healing tendon. Graphs showing **(a)** surrounding area adhesions, and **(b)** surrounding area vascularity 14 days postinjury, and **(c)** total cells after varying doses of BMP-12 released from mineral-coated suture or blank suture. Doses of 1.5 and 3.0 μg BMP-12 significantly reduced adhesions to the tendon **(a)**. Similarly, 1.5 μg BMP-12 significantly reduced the appearance of surrounding area adhesions **(b)**. A dose of 3.0 μg BMP-12 reduced total cell number within the healing tendon **(c)**. The *p*-value beneath the graph indicates ANOVA results. If ANOVA results were $p < 0.10$, Scheffe's *post hoc* pairwise analysis was performed. [a,b,c] Within a graph indicates *bars* without a common *superscript letter* differ ($p < 0.05$). Values are expressed as mean ranking ± S.E.M. * Indicates *p*-value = 0.0572.

### *Effects of 1.5 μg BMP-12 using different delivery methods*

The influence of treatments on tendon healing could be modulated by the type of vehicle used to deliver the growth factor. To determine if Achilles tendon healing was effected by delivery method, the 1.5 μg BMP-12 treatments were compared across methods (Fig. 6). Surrounding area adhesions and vascularity were substantially reduced after repair with BMP-12 delivered through the suture (adhesions, 0.0 ± 0.0 rank; vascularity, 1.83 ± 0.17 ranks) compared with BMP-12 injections (adhesions, 1.83 ± 0.17; vascularity, 3.00 ± 0.0 rank; Fig. 6a, b). BMP-12 delivered through collagen sponge also reduced adhesions (1.00 ± 0.0 rank) more than injections alone, but not to the degree of the sutures (Fig. 6a). The number of proliferating cells (118.58 ± 3.74 cells/mm$^2$; Fig. 6c) and blood vessel lumen (7.49 ± 0.51 lumen number/mm$^2$; Fig. 6d) were significantly increased after one injection of BMP-12 when compared with BMP-12-releasing sponges [proliferating cells, 88.71 ± 7.12 cells/mm$^2$; blood vessel lumen (2.73 ± 0.22 lumen number/mm$^2$)] or BMP-12-releasing sutures [proliferating cells, 54.20 ± 8.62 cells/mm$^2$; blood vessel lumen (4.08 ± 1.09 lumen number/mm$^2$)]. Myofibroblasts were significantly increased after repair with BMP-12-releasing sutures ($8.69 \pm 0.79 \times 10^{-3}$ density/mm$^2$) in comparison to sponge ($1.95 \pm 0.60 \times 10^{-3}$ density/mm$^2$) or injection ($4.20 \pm 0.72 \times 10^{-3}$ density/mm$^2$; Fig. 6e). Type III collagen ($p = 0.764$; Fig. 6f) and type I procollagen ($p = 0.537$; Fig. 6g) were not significantly different among delivery methods. Finally, collagen organization was similar after BMP-12 delivery by suture (1.86 ± < 0.01 fractal dimension; Fig. 6h) and sponge (1.86 ± 0.01 fractal dimension), and tended to be worse with BMP-12 injection (1.89 ± 0.01 fractal dimension). Based on these results, BMP-12 released from sutures was more effective at stimulating a response when compared with the standard delivery methods through collagen sponges or direct injections.

### *Substantiation of fractal analysis*

Previous studies indicated the use of multiphoton microscopy images to measure collagen organization through fractal analysis. To substantiate that H&E stained tissues can also serve as a source to quantify collagen organization through fractal analysis, normal healing tissue previously subjected to multiphoton microscopy and fractal analysis[28] was H&E stained and again subjected to fractal analysis. Similar to the previous multiphoton results,[28] H&E-stained tissue demonstrated that collagen organization significantly improved from day 5 to 28 (Fig. 7a, c) by its fractal dimension. This metric showed that organization was dissimilar to the intact tissue as expected. Additionally, curve fit data using a second-order polynomial equation, resulted an $R^2$ of 0.995 (Fig. 7b). These results suggest that fractal analysis may be used to successfully quantify collagen organization.

## Discussion

In contemporary regeneration and repair, a need exists for therapeutic protein release from common surgical devices,

TABLE 3. EFFECTS OF BMP-12 DELIVERED THROUGH COLLAGEN SPONGE OR DIRECT INJECTION ON MACROSCOPIC RANKINGS OF THE HEALING TENDON

| | *Sponge* | *BMP-12 sponge* | p-*Value* | *PBS injection* | *BMP-12 injection* | p-*Value* |
|---|---|---|---|---|---|---|
| Surrounding area adhesions (average ranking) | 2.5 ± 0.5 | 1.0 ± 0.0 | 0.040 | 1.33 ± 0.33 | 1.83 ± 0.17 | 0.251 |
| Surrounding area vascularity (average ranking) | 2.83 ± 0.17 | 2.50 ± 0.29 | 0.374 | 2.33 ± 0.17 | 3.00 ± 0.0 | 0.016 |
| Tendon inflammation (average ranking) | 2.0 ± 0.29 | 2.33 ± 0.33 | 0.492 | 1.50 ± 0.0 | 2.17 ± 0.17 | 0.016 |

BMP-12 added to a collagen sponge reduced adhesions, whereas BMP-12 injections increased the surrounding vascularity and tendon inflammation.

Table 4. Effects of BMP-12 Delivered Through Surgical Sutures on Cellular and Extracellular Matrix Factors by the Day 14 Healing Tendon

| *Total Achilles tendon* | *Blank* | *0.15 μg BMP-12* | *1.5 μg BMP-12* | *3.0 μg BMP-12* | p-*Value* |
|---|---|---|---|---|---|
| Proliferating cells (ave. cell number/mm$^2$) | 72.98 ± 4.59 | 72.33 ± 7.70 | 54.20 ± 8.65 | 74.81 ± 20.33 | 0.602 |
| Endothelial cells (ave. density/mm$^2$) × $10^{-3}$ | 2.01 ± 0.40 | 1.95 ± 0.13 | 2.24 ± 0.27 | 2.243 ± 0.27 | 0.829 |
| Blood vessel lumen (ave. lumen number/mm$^2$) | 2.87 ± 0.28 | 3.61 ± 0.53 | 4.08 ± 1.09 | 4.12 ± 0.73 | 0.617 |
| Myofibroblasts (ave. density/mm$^2$) × $10^{-3}$ | 4.17 ± 0.52 | 7.55 ± 0.45 | 8.69 ± 0.79 | 6.09 ± 1.42 | 0.082 |
| Type I procollagen (ave. density/mm$^2$) × $10^{-3}$ | 7.07 ± 2.33 | 1.90 ± 0.12 | 6.10 ± 3.41 | 1.97 ± 0.80 | 0.251 |
| Type III collagen (ave. density/mm$^2$) × $10^{-3}$ | 44.83 ± 3.00 | 54.87 ± 0.78 | 54.37 ± 2.88 | 54.37 ± 2.88 | 0.0658 |
| Collagen organization (ave. fractal dimension) | 1.85 ± 0.00 | 1.86 ± 0.00 | 1.86 ± 0.00 | 1.87 ± 0.01 | 0.129 |
| Normalized granulation tissue size (percent g.t. size) | 19.45 ± 3.14 | 24.53 ± 3.28 | 19.82 ± 3.20 | 24.47 ± 0.90 | 0.441 |

BMP-12-releasing sutures did not elicit a significant effect on the number of proliferating cells, endothelial cells, blood vessel lumen, type I procollagen, collagen organization, and granulation tissue size. Myofibroblasts and type III collagen *post hoc* analysis resulted in no significant differences. Values are expressed as means ± standard error of the mean.

g.t., granulation tissue.

to accelerate healing and ameliorate scar. To address this need, we examined mineral-coated sutures to locally release BMP-12 and compared the response to BMP-12 delivered from collagen sponge or BMP-12 direct injections for Achilles tendon healing. Our results indicate that (i) release of protein from mineral-coated sutures elicits a biological response; (ii) BMP-12 modulates some aspects of tendon healing; and (iii) the delivery method influences the tendon healing response to BMP-12.

A challenging problem, particularly with injured flexor tendons, is the formation of adhesions caused by tissue scarring around the tendon sheath. Although flexor tendons were not used in the current study, adhesions of the surrounding connective tissue to the Achilles tendon were evaluated at harvest. To our knowledge, the dose-dependent reduction in adhesions by BMP-12 when it was released from sutures or collagen sponges is a new finding. BMP-12 is a member of the TGF-β1 superfamily and TGF-β1 is a known modulator of collagen deposition and fibrosis. Although no previous research has indicated that BMP-12 is involved in regulating adhesions, research of other BMPs, including BMP-2,[35] -4,[35] and -7[35,36] has demonstrated their ability to reverse TGF-β1-induced epithelial–mesenchymal transition/endothelial–mesenchymal transition, respectively and fibrosis. Based on these results, adhesion formation may be modulated by balancing locally delivered BMP-12 (through sutures and collagen sponge) and TGF-β1 signaling.

All three delivery methods of BMP-12 modulated tendon healing, albeit in different manners. Of the three methods, 1.5 μg of BMP-12, delivered through mineral-coated sutures or collagen sponge, resulted in greater collagen organization and reduced adhesions (hallmarks of improved repair), compared with direct injections of BMP-12 at the same concentration. A previous study delivered 40–200 μg BMP-12 through collagen sponge to a periodontal defect and reported an improved functionally oriented ligament.[37] Another study injected 2.5 μg of BMP-12 to the injured Achilles tendon and noted increased cell numbers and tissue volume.[38] Despite the preclinical success using collagen sponges and injections as a delivery method, treatments are often required in supraphysiological doses and released in a poorly controlled manner. Indeed, in the aforementioned defects, changes in periodontal and Achilles tendon healing were noted after BMP-12 treatments of 40–200 μg[37] and 2.5 μg,[38] respectively. The use of mineral-coated sutures also allows for localized delivery without changing the standard surgical procedure. Because mineral is nucleated from an aqueous solution, mineral coating can be applied to

Table 5. Effect of BMP-12 Delivered Through Collagen Sponge or Injection on Cellular and Extracellular Matrix Factors by the Day 14 Healing Achilles Tendon

| | *Sponge* | *BMP-12 sponge* | p-*Value* | *PBS injection* | *BMP-12 injection* | p-*Value* |
|---|---|---|---|---|---|---|
| Total cells (ave. cell number/mm$^2$) | 804.19 ± 53.93 | 788.36 ± 9.50 | 0.787 | 880.81 ± 33.24 | 855.14 ± 85.64 | 0.794 |
| Proliferating cells (ave. cell number/mm$^2$) | 93.75 ± 19.80 | 88.71 ± 7.12 | 0.822 | 103.96 ± 14.08 | 118.58 ± 3.74 | 0.372 |
| Endothelial cells (ave. density/mm$^2$) × $10^{-3}$ | 2.85 ± 0.41 | 1.79 ± 0.53 | 0.189 | 3.86 ± 0.96 | 3.13 ± 0.42 | 0.521 |
| Blood vessel lumen (ave. lumen number/mm$^2$) | 3.21 ± 0.80 | 2.73 ± 0.22 | 0.598 | 4.23 ± 0.88 | 7.49 ± 0.51 | 0.033 |
| Myofibroblasts (ave. cell number/mm$^2$) × $10^{-3}$ | 6.34 ± 1.08 | 1.95 ± 0.60 | 0.58 | 9.35 ± 2.94 | 4.20 ± 0.72 | 0.165 |
| Type III collagen (ave. density/mm$^2$) × $10^{-3}$ | 40.17 ± 9.06 | 53.23 ± 3.88 | 0.256 | 52.47 ± 1.95 | 55.53 ± 4.13 | 0.539 |
| Type I procollagen (ave. density/mm$^2$) × $10^{-3}$ | 5.57 ± 3.54 | 4.33 ± 1.53 | 0.765 | 3.47 ± 1.50 | 2.43 ± 0.81 | 0.577 |
| Collagen organization (ave. fractal dimension) | 1.89 ± 0.01 | 1.86 ± 0.01 | 0.109 | 1.94 ± 0.02 | 1.89 ± 0.01 | 0.040 |
| Normalized granulation tissue size (percent g.t. size) | 33.16 ± 4.98 | 29.22 ± 3.94 | 0.569 | 33.10 ± 2.31 | 27.91 ± 2.31 | 0.187 |

Injection of BMP-12 significantly increased the number of blood vessel lumen and improved collagen organization. Values are expressed means ± standard error of the mean.

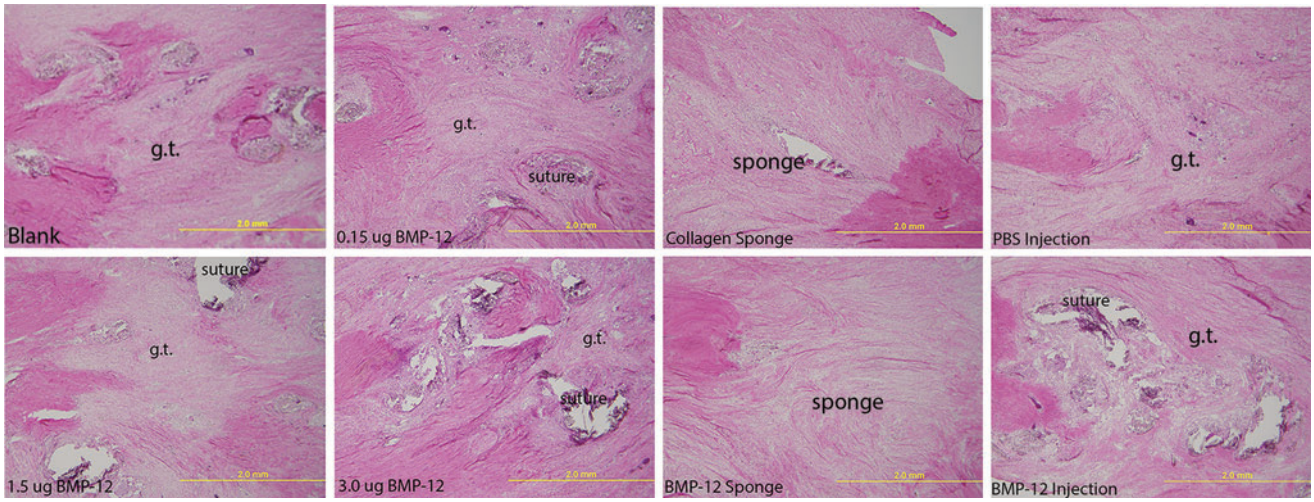


**FIG. 5.** Representative Hematoxylin and Eosin (H&E) micrographs of the granulation tissue after repair with the respective treatments. g.t., granulation tissue. Color images available online at www.liebertpub.com/tea

complex 3D structures/orthopedic implants and turn complicated structures into efficient growth factor delivery vehicles. Taken together, these results suggest that mineral coatings may provide an effective platform for efficient growth factor binding and release and subsequent biological response.

The use of mineral-coated sutures releasing basic fibroblast growth factor has previously been demonstrated in a sheep rotator cuff model.[5,9] The mineral coating served as a simple and highly adaptable carrier to bind and release proteins, which ultimately stimulated a biological response

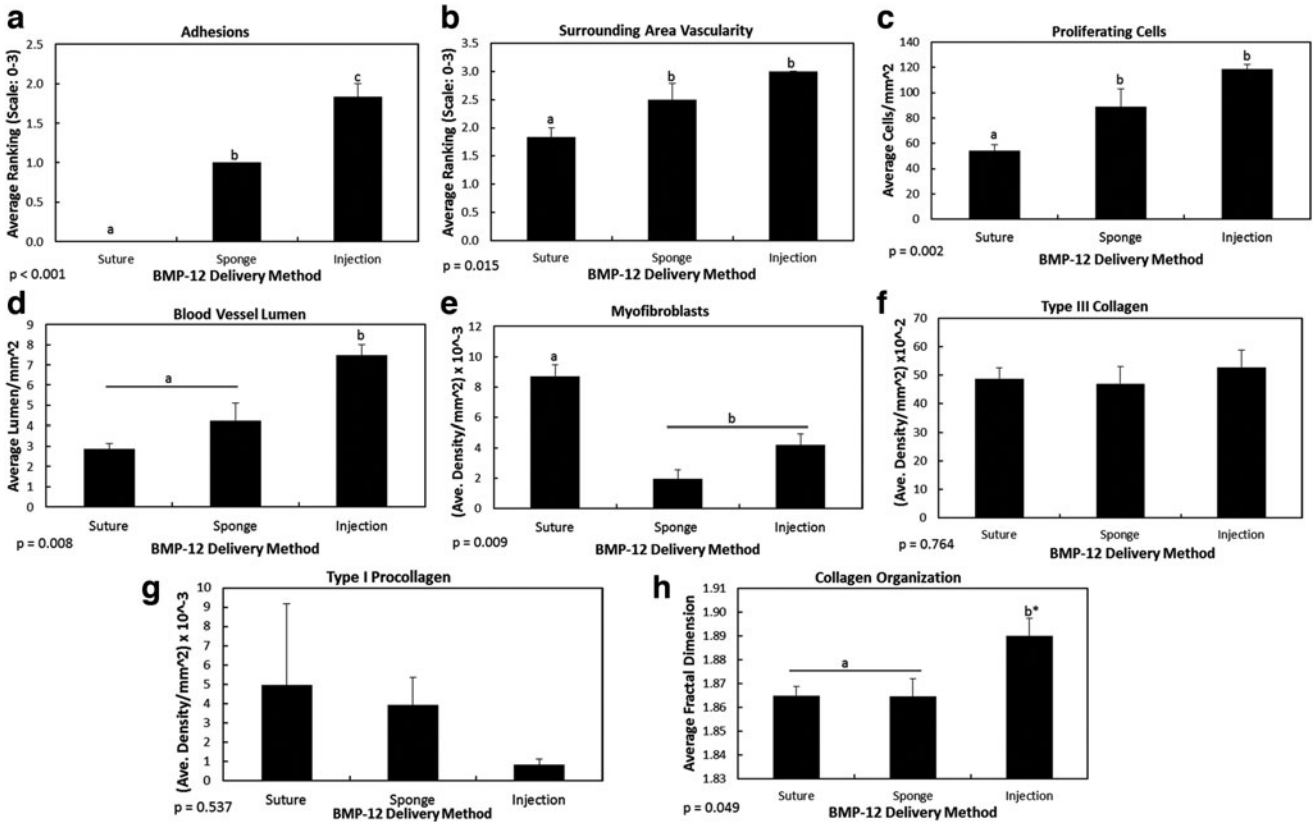


**FIG. 6.** Effects of 1.5 μg BMP-12 using different delivery methods. Comparison of BMP-12 delivered through suture, sponge, and injection on **(a)** surrounding area adhesions, **(b)** surrounding area vascularity, **(c)** proliferating cells, **(d)** blood vessel lumen, **(e)** myofibroblasts, **(f)** type III collagen, **(g)** type I procollagen, and **(h)** collagen organization. The *p*-value beneath the graph indicates ANOVA results. If ANOVA results were $p < 0.10$, Scheffe's *post hoc* pairwise analysis was performed. [a,b,c] Within a graph indicates *bars* without a common *superscript letter* differ ($p < 0.05$). Values are expressed as mean density ± S.E.M. *indicates *p*-value = 0.08.

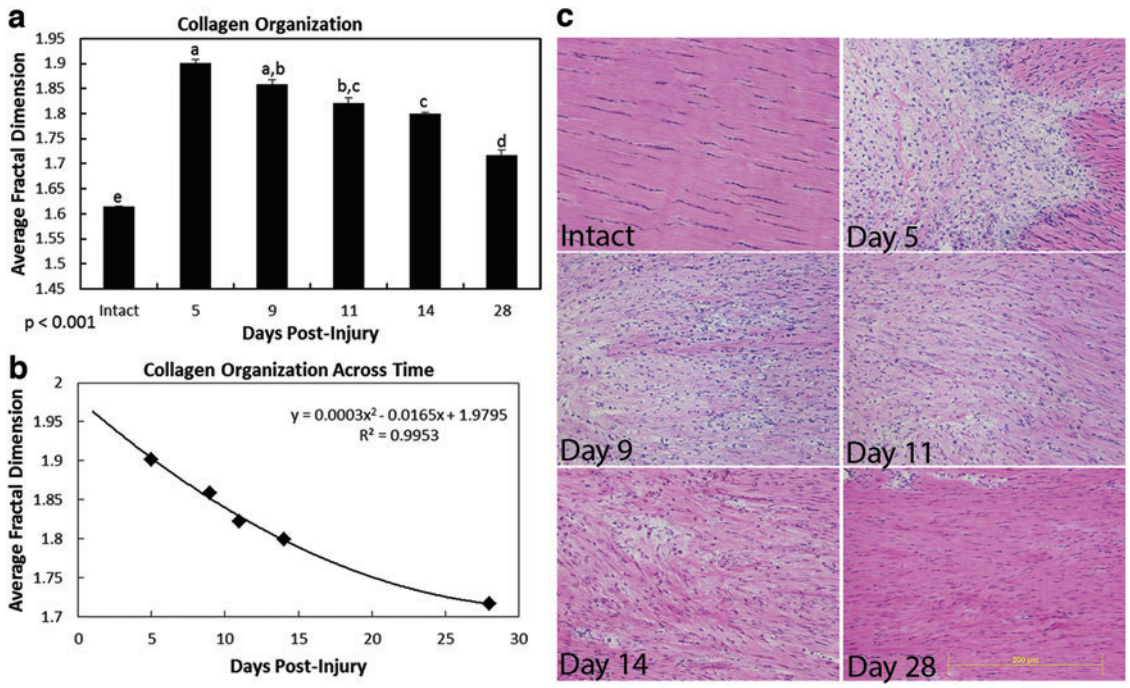


**FIG. 7.** Use of H&E-stained samples for collagen quantification through fractal analysis. Graph showing collagen organization of the normal healing (without treatment) rat medial collateral ligament (MCL) **(a)**. Intact tissue exhibits the greatest organization (i.e., lowest fractal dimension). Early ligament healing demonstrates significantly worse collagen organization (i.e., higher fractal dimension). By day 28, collagen organization has improved, but remains worse than the intact control. Graph demonstrating second-order polynomial curve fit of the normal healing results **(b)**. Representative H&E images of the intact, and day 5, 9, 11, 14, and 28 postinjured healing MCL used for fractal analysis **(c)**. The *p*-value beneath the graph indicates ANOVA results. If ANOVA results were $p < 0.10$, Scheffe's *post hoc* pairwise analysis was performed. $^{a,b,c,d,e}$ within a graph indicates *bars* without a common *superscript letter* differ ($p < 0.05$). Values are expressed as mean density ± S.E.M. Color images available online at www.liebertpub.com/tea

by the healing tendon. The current study further supports the use of mineral-coated sutures for BMP-12 release to modulate healing and repair. During tendon repair, BMP-12 is expressed during both early proliferation and later during remodeling.[38] Thus tendon regeneration may be enhanced by localized release of BMP-12 or other growth factors of interest. Considering the ubiquitous use of sutures and their location to damaged tissue, this approach may provide an efficient, site-specific method of regulating new tissue formation in numerous repair applications. Taken together, the results of this *in vivo* study indicate that CaP-coated BMP-12-releasing sutures can be used in a clinically relevant repair procedure.

The use of fractal analysis to quantify collagen organization has been previously demonstrated using multiphoton microscopy and SEM images of the ligament and tendon, respectively.[28] To our knowledge, this is the first study to demonstrate the successful use of fractal analysis on H&E stained tissue as an objective metric for tissue organization. Our results indicate that fractal analysis is capable of differentiating between healthy and healing or damaged collagenous tissue. Moreover, if a normal healing tissue is initially quantified over time, fractal analysis may be able to predict the healing day of a treated tissue, using the same healing model. Fractal analysis has the potential to significantly reduce the burden of subjectively quantifying collagen organization in damaged, diseased and healing tissues. This technique also provides potential value for other imaging modalities, including medical imaging within ultrasound or magnetic resonance imaging.

When interpreting these results, several issues must be borne in mind. First, the study did not perform any binding and release studies of BMP-12. However, prior studies from this lab performed extensive binding and release studies on a number of biomolecules and reported that protein binding capacity increased linearly with protein concentrations within an experimental range of 1.0–100 mg/mL for both acidic and basic proteins.[5,39] Moreover, no differences in release kinetics were observed between biomolecules when the total release amounts of biomolecule were converted into a percentage to the initially bound amount.[5] For instance, BMP-2 peptide showed gradual and sustained release over time, with ~80% of the initially bound biomolecule released during 6 weeks at a pH of 7.4.[39] Based on this information, we believe BMP-12 should bind and release similarly as our previously reported biomolecules. Second, we reported that BMP-12 dose dependently reduced adhesions in an Achilles tendon model rather than one known for adhesion problems such as the flexor tendon. The initial goal of this project was to identify any significant changes BMP-12 may have exerted on the Achilles tendon healing. We fortuitously found a change in adhesion formation during this study, but the effects of BMP-12 on adhesion formation in a study using flexor tendons is still required.

## Acknowledgments

The authors acknowledge Sarah Deunwald-Kuehl and Myranda L. Schmitt for fractal analysis, Samantha Pfeifer, Scott Liegel, Jake Zadra for capturing images and counting cells. BMP-12 was a generous gift from Pfizer (Cambridge, MA). Research reported in this publication was supported by the National Institute of Arthritis and Musculoskeletal and Skin Diseases of the National Institutes of Health under Award Number AR059916. The content is solely the responsibility of the authors and does not necessarily represent the official views of the National Institutes of Health.

## Disclosure Statement

No competing financial interests exist.

## References

1. Jeon, O., Song, S.J., Yang, H.S., *et al.* Long-term delivery enhances *in vivo* osteogenic efficacy of bone morphogenetic protein-2 compared to short-term delivery. Biochem Biophys Res Commun **369,** 774, 2008.
2. Kolambkar, Y.M., Boerckel, J.D., Dupont, K.M., *et al.* Spatiotemporal delivery of bone morphogenetic protein enhances functional repair of segmental bone defects. Bone **49,** 485, 2011.
3. Zhu, G., Mallery, S.R., and Schwendeman, S.P. Stabilization of proteins encapsulated in injectable poly (lactide-co-glycolide). Nat Biotechnol **18,** 52, 2000.
4. Zurita, R., Puiggali, J., and Rodriguez-Galan, A. Loading and release of ibuprofen in multi- and monofilament surgical sutures. Macromol Biosci **6,** 767, 2006.
5. Lee, J.S., Lu, Y., Baer, G.S., *et al.* Controllable protein delivery from coated surgical sutures. J Mater Chem **20,** 8894, 2010.
6. Dines, J.S., Weber, L., Razzano, P., *et al.* The effect of growth differentiation factor-5-coated sutures on tendon repair in a rat model. J Shoulder Elbow Surg **16,** 215s, 2007.
7. Hamada, Y., Katoh, S., Hibino, N., *et al.* Effects of monofilament nylon coated with basic fibroblast growth factor on endogenous intrasynovial flexor tendon healing. J Hand Surg Am **31A,** 530, 2006.
8. Rickert, M., Jung, M., Adiyaman, M., *et al.* A growth and differentiation factor-5 (GDF-5)-coated suture stimulates tendon healing in an Achilles tendon model in rats. Growth Factors **19,** 115, 2001.
9. Lu, Y.L., Nemke, J.S., Baer, B., Graf, G., Murphy, B.K., and Markel, M.D. Histologic evaluation of suture material loaded with basic fibroblast growth factor (bFGF) on acute rotator cuff repair in an ovine model. Curr Orthop Pract **22,** 425, 2011.
10. Gorbunoff, M.J. The interaction of proteins with hydroxyapatite. 1. Role of protein charge and structure. Anal Biochem **136,** 425, 1984.
11. Gorbunoff, M.J., and Timasheff, S.N. The interaction of proteins with hydroxyapatite. 3. Mechanism. Anal Biochem **136,** 440, 1984.
12. Bernardi, G., and Kawasaki, T. Chromatography of polypeptides and proteins on hydroxyapatite columns. Biochim Biophys Acta **160,** 301, 1968.
13. Bernardi, G. Chromatography of nucleic acids on hydroxyapatite. Nature **206,** 779, 1965.
14. Bernardi, G. Chromatography of nucleic acids on hydroxyapatite. I. Chromatography of native DNA. Biochim Biophys Acta **174,** 423, 1969.
15. Oda, S., Kinoshita, A., Higuchi, T., *et al.* Ectopic bone formation by biphasic calcium phosphate (BCP) combined with recombinant human bone morphogenetic protein-2 (rhBMP-2). J Med Dent Sci **44,** 53, 1997.
16. Lind, M., Overgaard, S., Ongipattanakul, B., *et al.* Transforming growth factor-beta 1 stimulates bone ongrowth to weight-loaded tricalcium phosphate coated implants—An experimental study in dogs. J Bone Joint Surg Br **78B,** 377, 1996.
17. Laffargue, P., Fialdes, P., Frayssinet, P., *et al.* Adsorption and release of insulin-like growth factor-I on porous tricalcium phosphate implant. J Biomed Mater Res **49,** 415, 2000.
18. Sogo, Y., Ito, A., Onoguchi, M., *et al.* Formation of a FGF-2 and calcium phosphate composite layer on a hydroxyapatite ceramic for promoting bone formation. Biomed Mater **2,** S175, 2007.
19. Kim, T.N., Feng, Q.L., Kim, J.O., *et al.* Antimicrobial effects of metal ions (Ag+, Cu2+, Zn2+) in hydroxyapatite. J Mater Sci Mater Med **9,** 129, 1998.
20. Blaker, J.J., Nazhat, S.N., and Boccaccini, A.R. Development and characterisation of silver-doped bioactive glass-coated sutures for tissue engineering and wound healing applications. Biomaterials **25,** 1319, 2004.
21. Ducy, P., and Karsenty, G. The family of bone morphogenetic proteins. Kidney Int **57,** 2207, 2000.
22. Wozney, J.M., and Rosen, V. Bone morphogenetic protein and bone morphogenetic protein gene family in bone formation and repair. Clin Orthop Relat Res **346,** 26, 1998.
23. Wolfman, N.M., Celeste, A.J., Cox, K., *et al.* Preliminary characterization of the biological-activities Rhbmp-12. J Bone Miner Res **10,** S148, 1995.
24. Wolfman, N.M., Hattersley, G., Cox, K., *et al.* Ectopic induction of tendon and ligament in rats by growth and differentiation factors 5, 6, and 7, members of the TGF-beta gene family. J Clin Invest **100,** 321, 1997.
25. Lou, J., Tu, Y., Burns, M., *et al.* BMP-12 gene transfer augmentation of lacerated tendon repair. J Orthop Res **19,** 1199, 2001.
26. Fu, S.C., Wong, Y.P., Chan, B.P., *et al.* The roles of bone morphogenetic protein (BMP) 12 in stimulating the proliferation and matrix production of human patellar tendon fibroblasts. Life Sci **72,** 2965, 2003.
27. Lu, Y., Lee, J.S., Nemke, B., *et al.* Coating with a modular bone morphogenetic peptide promotes healing of a bone-implant gap in an ovine model. PLoS One **7,** e50378, 2012.
28. Frisch, K.E., Duenwald-Kuehl, S.E., Kobayashi, H., *et al.* Quantification of collagen organization using fractal dimensions and Fourier transforms. Acta Histochem **114,** 140, 2012.
29. Moisy, F. Boxcount. Fractal dimension using the 'box-counting' method for 1D, 2D, and 3D sets. MATLAB Central, www.mathworks.com, 2008.
30. Chamberlain, C.S., Crowley, E.M., Kobayashi, H., *et al.* Quantification of collagen organization and extracellular matrix factors within the healing ligament. Microsc Microanal **17,** 779, 2011.
31. Jongpaiboonkit, L., Franklin-Ford, T., and Murphy, W.L. Growth of hydroxyapatite coatings on biodegradable polymer microspheres. ACS Appl Mater Interfaces **1,** 1504, 2009.
32. Suarez-Gonzalez, D., Barnhart, K., Saito, E., *et al.* Controlled nucleation of hydroxyapatite on alginate scaffolds

for stem cell-based bone tissue engineering. J Biomed Mater Res A **95,** 222, 2010.
33. Choi, S., and Murphy, W.L. Sustained plasmid DNA release from dissolving mineral coatings. Acta Biomater **6,** 3426, 2010.
34. Suarez-Gonzalez, D., Barnhart, K., Migneco, F., *et al.* Controllable mineral coatings on PCL scaffolds as carriers for growth factor release. Biomaterials **33,** 713, 2012.
35. Yang, Y.L., Ju, H.Z., Liu, S.F., *et al.* BMP-2 suppresses renal interstitial fibrosis by regulating epithelial-mesenchymal transition. J Cell Biochem **112,** 2558, 2011.
36. Zeisberg, E.M., Tarnavski, O., Zeisberg, M., *et al.* Endothelial-to-mesenchymal transition contributes to cardiac fibrosis. Nat Med **13,** 952, 2007.
37. Wikesjo, U.M.E., Sorensen, R.G., Kinoshita, A., *et al.* Periodontal repair in dogs: effect of recombinant human bone morphogenetic protein-12 (rhBMP-12) on regeneration of alveolar bone and periodontal attachment—A pilot study. J Clin Periodontol **31,** 662, 2004.
38. Jelinsky, S.A., Li, L., Ellis, D., *et al.* Treatment with rhBMP12 or rhBMP13 increase the rate and the quality of rat Achilles tendon repair. J Orthop Res **29,** 1604, 2011.
39. Lu, Y., Markel, M.D., Nemke, B., *et al.* Influence of hydroxyapatite-coated and growth factor-releasing interference screws on tendon-bone healing in an ovine model. Arthroscopy **25,** 1427–34.e1, 2009.

Address correspondence to:
*William L. Murphy, PhD*
*Department of Biomedical Engineering*
*University of Wisconsin*
*1111 Highland Avenue*
*WIMR Room 5405*
*Madison, WI 53705*

*E-mail:* wlmurphy@wisc.edu

*Ray Vanderby, PhD*
*Department of Biomedical Engineering*
*University of Wisconsin*
*1111 Highland Avenue*
*WIMR Room 5059*
*Madison, WI 53705*

*E-mail:* vanderby@ortho.wisc.edu

*Received: January 2, 2014*
*Accepted: October 3, 2014*
*Online Publication Date: December 10, 2014*